

# Catalysis Science & Technology

Volume 15  
Number 11  
7 June 2025  
Pages 3247–3454

rsc.li/catalysis



ISSN 2044-4761

Cite this: *Catal. Sci. Technol.*, 2025, 15, 3256Received 25th January 2025,  
Accepted 1st April 2025

DOI: 10.1039/d5cy00095e

rsc.li/catalysis

## Influence of H<sub>2</sub>-ICE specific exhaust conditions on the activity and stability of Cu-SSZ-13 deNO<sub>x</sub> catalysts†

Dhruba J. Deka, <sup>\*,a</sup> Garam Lee, <sup>a</sup> Kenneth G. Rappé, <sup>a</sup> Eric Walter, <sup>a</sup>  
Janos Szanyi <sup>a</sup> and Yong Wang <sup>ab</sup>

NO<sub>x</sub> abatement from H<sub>2</sub> internal combustion engines (H<sub>2</sub>-ICEs) is challenging due to high H<sub>2</sub>O content and unburned H<sub>2</sub> in the exhaust. This study examines Cu-SSZ-13 SCR catalysts, focusing on the effects of high H<sub>2</sub>O and H<sub>2</sub> levels on its activity and stability. High H<sub>2</sub>O content typical of H<sub>2</sub>-ICE exhaust hinders low-temperature SCR activity by impeding Cu migration and oxidation half cycle efficacy. H<sub>2</sub> slip decreases high-temperature SCR activity by reducing active Cu sites to the inactive Cu<sup>I</sup> state. Combined, high H<sub>2</sub>O and H<sub>2</sub> slip reduce SCR performance across all temperatures, making it less effective than in diesel applications. Additionally, aging under high H<sub>2</sub>O and H<sub>2</sub> contents induce a severe deterioration of Cu-SSZ-13 via CuO<sub>x</sub> formation and dealumination, further degrading catalyst performance. This suggests Cu-SSZ-13 may not be suitable for H<sub>2</sub>-ICE aftertreatment, especially given the ongoing development of H<sub>2</sub>-ICE itself. Parallel efforts in H<sub>2</sub>-ICE and catalyst development are essential to accelerate H<sub>2</sub>-ICE deployment.

Use of hydrogen in internal combustion engines (ICEs) has recently garnered significant attention, especially for heavy-duty machinery and vehicles.<sup>1,2</sup> Along with being a low-to-zero carbon strategy, H<sub>2</sub>-ICEs also offer higher power output and thermal efficiency than traditional fossil fuel ICEs.<sup>3</sup> The major pollutants emitted by H<sub>2</sub>-ICEs are oxides of nitrogen (NO<sub>x</sub>: NO, NO<sub>2</sub>, N<sub>2</sub>O).

Copper-exchanged small pore zeolite Cu-SSZ-13 is a state-of-the-art catalyst used in diesel exhaust aftertreatment to remove NO<sub>x</sub> via selective catalytic reduction (SCR) with NH<sub>3</sub> (4NO + 4NH<sub>3</sub> + O<sub>2</sub> → 4N<sub>2</sub> + 6H<sub>2</sub>O).<sup>4</sup> Years of research have provided a detailed understanding of the reaction mechanisms of these

catalysts under typical diesel-ICE exhaust conditions.<sup>5–9</sup> These studies have identified isolated Cu sites in two geometries as active sites for SCR: (1) Z<sub>1</sub>CuOH where Cu-ions are coordinated with a single framework Al in 8-membered rings (MR), and (2) Z<sub>2</sub>Cu where they are coordinated with two Al sites in 6MRs. The SCR reaction cycles Cu sites between Cu<sup>II</sup> and Cu<sup>I</sup> states through reduction and oxidation half-cycles (RHC and OHC). However, little is known about the behavior of these active sites and their stability in H<sub>2</sub>-ICE exhaust, which is characterized by high H<sub>2</sub>O content (up to 25 vol%) and the likely presence of unburned H<sub>2</sub>.<sup>10</sup> Such information gap must be addressed to determine whether Cu-SSZ-13 is viable for H<sub>2</sub>-ICEs, or if alternative catalysts should be developed. This study offers a crucial step towards closing this gap.

Here, we conducted detailed activity measurements and electron paramagnetic resonance (EPR) spectroscopy characterization of a commercially relevant Cu-SSZ-13 catalyst in simulated H<sub>2</sub>-ICE exhaust, containing high H<sub>2</sub>O content (up to 20%) and H<sub>2</sub> (up to 4000 ppm). Details on experimental setup and methods are provided in ESI† (Note S1).

We first focused on the impact of H<sub>2</sub>O content (0, 3, 6, 10, and 20 vol%) on NO<sub>x</sub> conversion efficiency, presented in Fig. 1a, with low-temperature data (100–300 °C) replotted in Fig. S1.† Compared to dry conditions, 3% H<sub>2</sub>O significantly increased NO<sub>x</sub> conversion at ≥280 °C and moderately increased it below this temperature, particularly above 150 °C. The improvement at >280 °C is primarily due to decreased parasitic NH<sub>3</sub> oxidation, as evident from NH<sub>3</sub> oxidation activity in Fig. S2† and a decreased N<sub>2</sub>O production at temperatures >300 °C.<sup>11</sup> H<sub>2</sub>O competes for active Cu sites (confirmed by NH<sub>3</sub> adsorption data in Fig. S3†), reducing their ability to oxidize NH<sub>3</sub>, which in turn improves NH<sub>3</sub> utilization in the SCR reaction. At <280 °C, the mechanisms by which H<sub>2</sub>O promotes NO<sub>x</sub> conversion are complex and multi-faceted. Ma *et al.* showed that H<sub>2</sub>O promotes surface nitrates and NO<sub>2</sub> formation at temperatures >250 °C which

<sup>a</sup> Institute for Integrated Catalysis, Pacific Northwest National Laboratory, Richland, WA 99354, USA. E-mail: dhrubajyoti.deka@pnnl.gov

<sup>b</sup> The Gene and Linda Voiland School of Chemical Engineering and Bioengineering, Washington State University, Pullman, WA 99163, USA

† Electronic supplementary information (ESI) available. See DOI: <https://doi.org/10.1039/d5cy00095e>



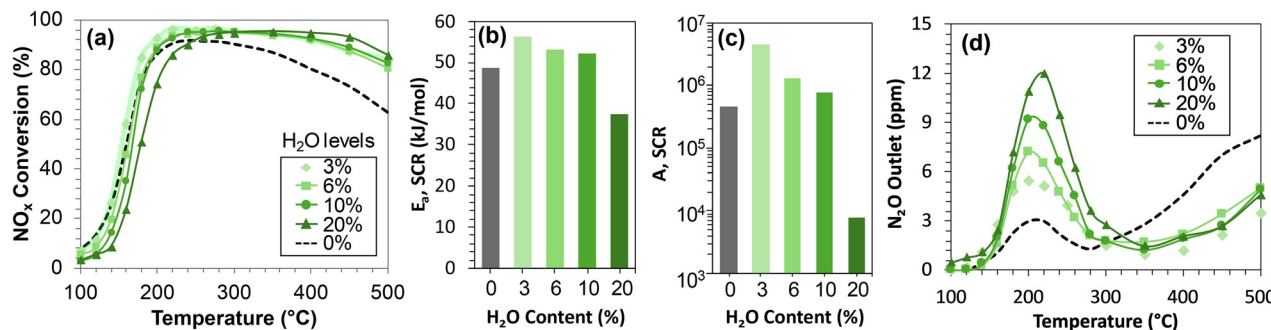


Fig. 1 (a) Steady state standard SCR  $\text{NO}_x$  conversion at different feed  $\text{H}_2\text{O}$  content (0, 3, 6, 10, 20%) on Cu-SSZ-13, (b) SCR activation energy, (c) SCR pre-exponential factor, (d)  $\text{N}_2\text{O}$  byproduct formation during SCR.

then react with Brønsted acid bound  $\text{NH}_3$ , leading to improved  $\text{NO}_x$  conversion.<sup>12</sup> The SCR performance below 280 °C is greatly affected by the migration and hydrolysis of active Cu centers. Utilizing *in situ* DRIFTS and XANES, Lee *et al.* concluded that  $\text{H}_2\text{O}$  promotes the mobility of  $\text{Cu}^{\text{I}}$  ions during the OHC.<sup>13</sup> In addition, Hu *et al.*<sup>14</sup> and Wu *et al.*<sup>15</sup> showed that  $\text{H}_2\text{O}$  facilitates hydrolysis of  $\text{Cu}^{\text{II}}(\text{NH}_3)_4$  intermediates to more reactive  $\text{Cu}^{\text{II}}(\text{OH})(\text{NH}_3)_3$  species, which improves  $\text{Cu}^{\text{II}}$  mobility and allows formation of two-proximate  $\text{Cu}^{\text{II}}$  configuration, thereby promoting the RHC. Consequently, it is likely that the improved low-temperature SCR activity under 3%  $\text{H}_2\text{O}$  versus dry conditions is due to enhanced OHC and RHC facilitated by improved  $\text{Cu}^{\text{I}}/\text{Cu}^{\text{II}}$  migration and  $\text{Cu}^{\text{II}}$  hydrolysis.  $\text{H}_2\text{O}$ -induced promotion of both half cycles was also reported by Nasello *et al.*<sup>16</sup>

However,  $\text{NO}_x$  conversion behavior and the interaction of  $\text{H}_2\text{O}$  at low temperature is not altogether straightforward. Ottinger *et al.* observed a positive impact of  $\text{H}_2\text{O}$  on  $\text{NO}_x$  conversion at  $\text{NO}_x > 200$  ppm but a negative impact at lower concentrations.<sup>17</sup> While we did not change feed  $\text{NO}_x$  in our experiments, variations in  $\text{H}_2\text{O}$  content were investigated. As seen in Fig. 1a and S1,† low-temperature  $\text{NO}_x$  conversion decreases with increased  $\text{H}_2\text{O}$  concentration above 3%. For instance, at 20%  $\text{H}_2\text{O}$ , representative of  $\text{H}_2$ -ICE exhaust,  $\text{NO}_x$  conversion at 200 °C is only 74% compared to 93% with 3%  $\text{H}_2\text{O}$  present. The low-temperature  $\text{NO}_x$  conversion data were used in Arrhenius analysis, yielding the  $\ln(k)$  vs.  $1/T$  plots shown in Fig. S4a.† The SCR activation energy ( $E_a$ ) and pre-exponential factors ( $A$ ) were calculated at varying  $\text{H}_2\text{O}$  contents. Previous studies have established that SCR with RHC as the rate limiting half cycle has an  $E_a$  of  $\sim 80$   $\text{kJ mol}^{-1}$ , while an OHC-limited SCR has  $E_a$  of  $\sim 35$   $\text{kJ mol}^{-1}$ .<sup>6,18</sup> As seen in Fig. 1b and c, the  $E_a$  and  $A$  values increases from dry to 3–10%  $\text{H}_2\text{O}$ , which is attributed to improved  $\text{Cu}^{\text{I}}$  mobility and  $\text{O}_2$  activation on Cu-dimers.<sup>13,15</sup> These factors shift the SCR kinetics away from OHC-limited regime, which increases the  $E_a$  and  $A$ . An activation energy between 50–60  $\text{kJ mol}^{-1}$  indicates both half cycles are kinetically relevant. However, both  $E_a$  and  $A$  decrease at 20%  $\text{H}_2\text{O}$ , indicating SCR becomes OHC-limited at high  $\text{H}_2\text{O}$  levels. The  $A$  value is nearly three orders of magnitude lower at 20%  $\text{H}_2\text{O}$  compared to 3%  $\text{H}_2\text{O}$ . Such low  $A$  indicates less efficient collisions between

reactants and active Cu sites. Millan *et al.* observed in a recent DFT study that the activation barrier for  $\text{Cu}^{\text{I}}(\text{NH}_3)_2$  inter-cage diffusion increases in the presence of excess  $\text{H}_2\text{O}$  molecules within zeolite cages.<sup>19</sup> This hindered diffusion would reduce the likelihood of  $\text{Cu}(\text{NH}_3)_2\text{-O}_2\text{-Cu}(\text{NH}_3)_2$  dimer formation, necessary to facilitate the OHC, thus decreasing SCR efficiency which aligns with our findings. Hence, while a small amount of  $\text{H}_2\text{O}$  can enhance SCR activity by improving Cu mobility and hydrolysis, excess  $\text{H}_2\text{O}$  on the other hand could reduce SCR performance by impeding Cu movement.

Additionally, water content in the simulated  $\text{H}_2$ -ICE exhaust also impacts Cu-SSZ-13 SCR selectivity at low temperatures. Fig. 1d and S4b† show nitrous oxide ( $\text{N}_2\text{O}$ ) byproduct formation and  $\text{N}_2\text{O}$  selectivity from Cu-SSZ-13 during SCR at various  $\text{H}_2\text{O}$  levels. The differences in  $\text{N}_2\text{O}$  formation with and without water at  $>280$  °C are attributed to  $\text{NH}_3$  oxidation.<sup>11</sup> However, below 280 °C,  $\text{N}_2\text{O}$  formation increases with  $\text{H}_2\text{O}$  content. At 20%  $\text{H}_2\text{O}$ , typical of  $\text{H}_2$ -ICE exhaust,  $\text{N}_2\text{O}$  levels are twice as high compared to those at 6%  $\text{H}_2\text{O}$ , typical of diesel exhaust. This is concerning because  $\text{N}_2\text{O}$  has a global warming potential  $\sim 300$  times greater than  $\text{CO}_2$ .<sup>20</sup> Increased  $\text{N}_2\text{O}$  selectivity likely arises, at least in part, from hindered inter-cage diffusion of  $\text{Cu}^{\text{I}}(\text{NH}_3)_2$  species, making them more prone to non-SCR reaction pathways. Our ongoing efforts focus on uncovering the exact mechanism behind  $\text{H}_2\text{O}$ -promotion of  $\text{N}_2\text{O}$  formation, which will be addressed in future publications.

We now focus on the impact of  $\text{H}_2$  on the  $\text{NO}_x$  conversion efficiency on Cu-SSZ-13. To simulate SCR performance in the presence of  $\text{H}_2$  slip from the ICE (*i.e.*, unburned  $\text{H}_2$ ), experiments were conducted to measure  $\text{NO}_x$  conversion in a feed containing 20%  $\text{H}_2\text{O}$  with 200, 1000, and 4000 ppm  $\text{H}_2$ . These results are shown in Fig. 2a combined with  $\text{NO}_x$  conversion performance with 20%  $\text{H}_2\text{O}$  without  $\text{H}_2$  previously shown. The presence of  $\text{H}_2$  with 20%  $\text{H}_2\text{O}$  decreases  $\text{NO}_x$  conversion by up to 10% at  $>200$  °C, with this effect being relatively insensitive to the level of  $\text{H}_2$  within the range studied. This temperature range where  $\text{NO}_x$  conversion decreases align well with the range where  $\text{H}_2$  conversion takes place on Cu-CHA (Fig. S5†). Additionally,  $\text{H}_2$ -temperature programmed reduction ( $\text{H}_2$ -TPR) of Cu-SSZ-13





Fig. 2 (a) Steady-state SCR NO<sub>x</sub> conversion under 0, 200 ppm, 1000 ppm, and 4000 ppm H<sub>2</sub>, (b) H<sub>2</sub>-TPR of Cu-SSZ-13, (c) NO transient during SCR at 250 °C with and without 200 ppm H<sub>2</sub>.

catalyst, as shown in Fig. 2b, indicates that Cu sites reduce from Cu<sup>II</sup> to Cu<sup>I</sup> under H<sub>2</sub> at >200 °C. It is likely that under SCR conditions, H<sub>2</sub> has a similar reducing effect, creating a steady-state pool of Cu<sup>I</sup> sites that do not participate in SCR redox activities. Although O<sub>2</sub> is present in the reaction mixture, a decreased NO<sub>x</sub> conversion and an incomplete H<sub>2</sub> conversion (Fig. S5†) implies that Cu<sup>II</sup> reduction by H<sub>2</sub> to Cu<sup>I</sup> is faster than Cu<sup>I</sup> re-oxidation by O<sub>2</sub>.

To further elucidate the impact of H<sub>2</sub> on Cu-SSZ-13 SCR performance, Fig. 2c presents reactor outlet NO concentration with and without 200 ppm H<sub>2</sub> at 250 °C, and Fig. S6a† shows analogous results at 1000 and 4000 ppm H<sub>2</sub>. Initially without H<sub>2</sub>, ~26 ppm NO was measured. When H<sub>2</sub> is introduced at ~2800 s, an NO spike to 600 ppm is observed, after which a

steady state is reached at ~37 ppm NO. This spike in NO can be directly attributed to H<sub>2</sub> reducing a portion of Cu<sup>II</sup> sites to Cu<sup>I</sup>, leading to the rapid desorption of NO<sub>x</sub> species previously bound to Cu<sup>II</sup>. Adsorbed nitrate species form at temperatures >250 °C due to an increased NO oxidation activity.<sup>21</sup> The subsequent higher steady state NO outlet is the result of H<sub>2</sub> shifting the Cu inventory preferentially to Cu<sup>I</sup>, thus impeding the effective redox capacity of the catalyst. Next, when H<sub>2</sub> is turned off at ~4300 s, NO concentration drops to 0 ppm for a while (through ~5000 s) before it slowly returns to the original 26 ppm value observed at the start of the test. This NO consumption occurs due to the accelerated (re)oxidation of Cu<sup>I</sup> to Cu<sup>II</sup> when H<sub>2</sub> is removed, thereby leading to (re)adsorption of NO<sub>x</sub> species. Fig. S6b† shows the integrated quantities NO desorbed with H<sub>2</sub> introduction and NO adsorbed with H<sub>2</sub> removal. These results show that the quantities of NO desorbed and adsorbed at 200, 1000, and 4000 ppm H<sub>2</sub> are very similar. Consistent N<sub>2</sub>O production during the SCR reaction tests with H<sub>2</sub>, as presented in Fig. S7,† indicates no influence of H<sub>2</sub> on N<sub>2</sub>O selectivity; this is expected since H<sub>2</sub> has minimal impact on low-temperature SCR activity.

Finally, the stability of Cu-SSZ-13 samples in the presence of high H<sub>2</sub>O and H<sub>2</sub> was investigated by hydrothermally aging them under three different environments, followed by testing under standard SCR conditions with 6% H<sub>2</sub>O and no H<sub>2</sub>. HTA-1 was aged under 6% H<sub>2</sub>O to provide a reference to diesel exhaust conditions, HTA-2 was aged under 20% H<sub>2</sub>O to assess the impact of high-water content, and HTA-3 was aged under 20% H<sub>2</sub>O + 1000 ppm H<sub>2</sub> to assess the impact of both high-water content and H<sub>2</sub> slip. All aging treatments were done at 650 °C for 50 hours with air as the balance gas, and the subsequent NO<sub>x</sub> conversion results on these samples under 6% H<sub>2</sub>O are shown in Fig. 3a. As expected, HTA-1 exhibits decreased NO<sub>x</sub> conversion at <350 °C versus the fresh sample (FR) with little impact at high temperature; this can be attributed to the conversion of a portion of Z<sub>1</sub>CuOH sites to Z<sub>2</sub>Cu and concomitant depletion of Brønsted acid sites.<sup>22</sup> HTA-2 shows a modest further decrease in low-temperature activity along with markedly lower high-temperature NO<sub>x</sub> conversion compared to HTA-1. Decreases in both high- and low-temperature NO<sub>x</sub> conversions indicate that along with Z<sub>1</sub>CuOH to Z<sub>2</sub>Cu conversion, the HTA-2 sample also forms CuO<sub>x</sub> particles (evident from EPR discussed below), increasing the magnitude of non-selective NH<sub>3</sub> oxidation, thereby decreasing the SCR activity.

HTA-3 shows similar high-temperature performance as HTA-2 (attributed to CuO<sub>x</sub> particles) but significantly reduced low-temperature NO<sub>x</sub> conversion. These results suggest that the presence of H<sub>2</sub> along with H<sub>2</sub>O during aging has a detrimental effect on the stability of Cu-SSZ-13 catalysts that is not solely attributed to CuO<sub>x</sub> particle formation. To further elucidate the impact of aging conditions on Cu-SSZ-13, the E<sub>a</sub> and A of low-temperature SCR on the aged catalysts are tabulated inside Fig. 3a, providing two important insights: (1) similar activation energies for all catalysts indicate the same SCR reaction mechanism and rate-determining step, and (2)





**Fig. 3** (a) SCR NO<sub>x</sub> conversion on four Cu-SSZ-13 samples with varied aging treatment: FR, HTA-1, HTA-2, HTA-3. (b) X-band EPR spectra of FR, HTA-1, HTA-2 and HTA-3 samples. Insets show ratios of total EPR signal relative to FR and high field region of HTA-3. (c) N<sub>2</sub>O byproduct formation during SCR.

a strikingly lower pre-exponential factor for HTA-3 suggests a pronounced decrease in active Cu sites. To confirm this, we used EPR to determine the speciation and concentration of isolated Cu ions, widely regarded as the primary active sites for the SCR reaction. Fig. 3b shows the *ex situ* EPR spectra of hydrated FR, HTA-1, HTA-2, and HTA-3 at  $-150$  °C. The high-field EPR regions of FR, HTA-1, and HTA-2 show a consistent single peak at  $g_{||} = 2.07$  attributed to anisotropic Cu<sup>II</sup> ions typical of Cu-SSZ-13 (more details in ESI† Fig. S8).<sup>18</sup> The loss of isolated Cu sites to CuO<sub>x</sub> clusters (which are not EPR active) is reflected in a decreased overall EPR signal. As shown in Fig. S8† the total EPR signal of HTA-1 is similar to that of FR, confirming negligible CuO<sub>x</sub> formation at 6% H<sub>2</sub>O (typical of diesel exhaust conditions). HTA-2 also shows similar EPR patterns but with ~24% decreased EPR signal, confirming that high H<sub>2</sub>O content increases CuO<sub>x</sub>, leading to

decreased performance. The EPR spectra of HTA-3, however, is notably different, with significant reductions in both the hyperfine and high-field regions. The high-field region shows features at  $g_{||} = 2.05$  and  $g_{||} = 2.03$ , which Wang *et al.* identified as belonging to CuAl<sub>2</sub>O<sub>4</sub> species.<sup>23</sup> Since H<sub>2</sub> is oxidized over Cu sites (Fig. S5†), the ensued exothermicity may lead to a reaction between Cu and Al to form CuAl<sub>2</sub>O<sub>4</sub>-type species. This indicates that the presence of H<sub>2</sub> and high H<sub>2</sub>O content, typical of H<sub>2</sub>-ICE exhaust conditions during hydrothermal aging, leads to a significant loss of isolated Cu (~72% based on Fig. S8†). Some of the lost Cu exits the zeolite framework, interacts with Al, and causes dealumination, leading to the formation of CuAl<sub>2</sub>O<sub>4</sub>. While CuO<sub>x</sub> particles could still assist low-temperature SCR activity by oxidizing NO to form NO<sub>2</sub> *in situ*, facilitating the fast-SCR reaction, CuAl<sub>2</sub>O<sub>4</sub> does not, resulting in a significant decrease in low-temperature SCR activity on HTA-3.

The detrimental impact of H<sub>2</sub>-ICE exhaust goes beyond decreased SCR activity and the loss of active Cu sites; it also affects N<sub>2</sub>O formation. As shown in Fig. 3c, HTA-3 generates significantly more N<sub>2</sub>O compared to the other samples. The exact cause of N<sub>2</sub>O formation remains unclear, whether it stems from reduced OHC efficacy or the formation of CuO<sub>x</sub> or CuAl<sub>2</sub>O<sub>4</sub> species. Nevertheless, it is evident that HTA-3 degradation due to high H<sub>2</sub>O content and H<sub>2</sub> increases harmful N<sub>2</sub>O emissions at both low and high temperatures.

In summary, this study evaluates the feasibility of Cu-SSZ-13 as an NH<sub>3</sub>-SCR deNO<sub>x</sub> catalyst under in H<sub>2</sub>-ICE exhaust conditions. The high H<sub>2</sub>O concentration typical of H<sub>2</sub>-ICE exhaust reduces low-temperature SCR activity by hindering Cu migration and limiting the oxidation half-cycle efficacy. Additionally, H<sub>2</sub> slip decreases high-temperature SCR activity by converting active Cu sites to the inactive Cu<sup>I</sup> state. Our findings show that the simultaneous presence of high H<sub>2</sub>O and unburned H<sub>2</sub> significantly decreases the SCR performance of Cu-SSZ-13 across the entire temperature range when compared to diesel exhaust. Hydrothermal aging under high H<sub>2</sub>O results in a noticeable decrease in isolated Cu sites due to increased CuO<sub>x</sub> formation. Moreover, the co-presence of high H<sub>2</sub>O and H<sub>2</sub> causes severe deterioration of Cu-SSZ-13, including dealumination and the formation of inactive CuO<sub>x</sub> and CuAl<sub>2</sub>O<sub>4</sub> species. This evidence suggests that Cu-SSZ-13 may not be a suitable SCR catalyst for H<sub>2</sub>-ICE applications. Molecular level understanding of these observations will be key to developing the next generation of SCR catalysts optimized for H<sub>2</sub>-ICE applications. Reducibility of different isolated Cu species (Z<sub>1</sub>CuOH *vs.* Z<sub>2</sub>Cu) and changes in support acidity caused by Si/Al ratio and topology differences should be exploited to design new catalysts. The development of more resilient catalysts is further complicated by the evolving nature of H<sub>2</sub>-ICE technology, with variables like NO<sub>x</sub> levels, unburned H<sub>2</sub>, and exhaust temperature still largely undefined. Therefore, maintaining open communication between catalyst developers and OEMs will be crucial for the successful deployment of H<sub>2</sub>-ICE technologies.



## Data availability

The data supporting this article have been included as part of the manuscript and ESI.†

## Author contributions

D. J. Deka: investigation, data curation, writing – original draft. G. Lee: investigation, data curation, writing – review and editing. K. Rappe: conceptualization, supervision, funding acquisition, writing – review & editing. E. Walter: investigation, writing – review & editing. J. Szanyi: supervision, writing – review and editing. Y. Wang: conceptualization, supervision, funding acquisition, writing – review and editing.

## Conflicts of interest

There are no conflicts to declare.

## Acknowledgements

The authors from Pacific Northwest National Laboratory (PNNL) gratefully acknowledge the US Department of Energy (DOE), Energy Efficiency and Renewable Energy, Vehicle Technologies Office for the support of this work. Part of the research described in this paper was performed in the Environmental Molecular Sciences Laboratory (EMSL), a national scientific user facility sponsored by the DOE's Office of Biological and Environmental Research and located at PNNL. PNNL is operated for the US DOE by Battelle under contract number DE-AC05-76RL01830.

## Notes and references

- 1 C. Bekdemir, E. Doosje and X. Seykens, *H2-ICE Technology Options of the Present and the Near Future*, SAE Technical Paper, 2022.
- 2 A. Onorati, R. Payri, B. Vaglieco, A. K. Agarwal, C. Bae, G. Bruneaux, M. Canakci, M. Gavaises, M. Gunthner and C. Hasse, The role of hydrogen for future internal combustion engines, *Int. J. Engine Res.*, 2022, **23**, 529–540.
- 3 J. Nieminen and I. Dincer, Comparative exergy analyses of gasoline and hydrogen fuelled ICEs, *Int. J. Hydrogen Energy*, 2010, **35**(10), 5124–5132.
- 4 A. M. Beale, F. Gao, I. Lezcano-Gonzalez, C. H. Peden and J. Szanyi, Recent advances in automotive catalysis for NO<sub>x</sub> emission control by small-pore microporous materials, *Chem. Soc. Rev.*, 2015, **44**(20), 7371–7405.
- 5 F. Gao, D. Mei, Y. Wang, J. Szanyi and C. H. Peden, Selective Catalytic Reduction over Cu/SSZ-13: Linking Homo- and Heterogeneous Catalysis, *J. Am. Chem. Soc.*, 2017, **139**(13), 4935–4942, DOI: [10.1021/jacs.7b01128](https://doi.org/10.1021/jacs.7b01128) From NLM PubMed-not-MEDLINE.
- 6 C. Paolucci, I. Khurana, A. A. Parekh, S. Li, A. J. Shih, H. Li, J. R. Di Iorio, J. D. Albarracin-Caballero, A. Yezerets and J. T. Miller, Dynamic multinuclear sites formed by mobilized copper ions in NO<sub>x</sub> selective catalytic reduction, *Science*, 2017, **357**(6354), 898–903.
- 7 D. J. Deka, R. Daya, S. Y. Joshi and W. P. Partridge, On the various Cu-redox pathways and O<sub>2</sub>-mediated Bronsted-to-Lewis adsorbed-NH<sub>3</sub> redistribution under SCR half-cycle conditions, *Appl. Catal., A*, 2022, **640**, 118656.
- 8 W. Hu, T. Selli, F. Gramigni, E. Fenes, K. R. Rout, S. Liu, I. Nova, D. Chen, X. Gao and E. Tronconi, On the redox mechanism of low-temperature NH<sub>3</sub>-SCR over Cu-CHA: a combined experimental and theoretical study of the reduction half cycle, *Angew. Chem., Int. Ed.*, 2021, **60**(13), 7197–7204.
- 9 K. Khivantsev, J.-H. Kwak, N. R. Jaegers, I. Z. Koleva, G. N. Vayssilov, M. A. Derewinski, Y. Wang, H. A. Aleksandrov and J. Szanyi, Identification of the mechanism of NO reduction with ammonia (SCR) on zeolite catalysts, *Chem. Sci.*, 2022, **13**(35), 10383–10394.
- 10 İ. A. Reşitoğlu, K. Altinişik and A. Keskin, The pollutant emissions from diesel-engine vehicles and exhaust aftertreatment systems, *Clean Technol. Environ. Policy*, 2015, **17**, 15–27.
- 11 J. Yang, S. Ren, Z. Su, L. Yao, J. Cao, L. Jiang, G. Hu, M. Kong, J. Yang and Q. Liu, *In situ* IR comparative study on N<sub>2</sub>O formation pathways over different valence states manganese oxides catalysts during NH<sub>3</sub>-SCR of NO, *Chem. Eng. J.*, 2020, **397**, 125446.
- 12 L. Ma, Z. Li, H. Zhao, T. Zhang, N. Yan and J. Li, Understanding the Water Effect for Selective Catalytic Reduction of NO<sub>x</sub> with NH<sub>3</sub> over Cu-SSZ-13 Catalysts, *ACS ES&T Eng.*, 2022, **2**(9), 1684–1696.
- 13 H. Lee, R. J. G. Nuguid, S. W. Jeon, H. S. Kim, K. H. Hwang, O. Kröcher, D. Ferri and D. H. Kim, *In situ* spectroscopic studies of the effect of water on the redox cycle of Cu ions in Cu-SSZ-13 during selective catalytic reduction of NO<sub>x</sub>, *Chem. Commun.*, 2022, **58**(46), 6610–6613.
- 14 W. Hu, U. Iacobone, F. Gramigni, Y. Zhang, X. Wang, S. Liu, C. Zheng, I. Nova, X. Gao and E. Tronconi, Unraveling the hydrolysis of Z<sub>2</sub>Cu<sup>2+</sup> to ZCu<sup>2+</sup>(OH)<sup>-</sup> and its consequences for the low-temperature selective catalytic reduction of NO on Cu-CHA catalysts, *ACS Catal.*, 2021, **11**(18), 11616–11625.
- 15 Y. Wu, W. Zhao, S. H. Ahn, Y. Wang, E. D. Walter, Y. Chen, M. A. Derewinski, N. M. Washton, K. G. Rappe and Y. Wang, *et al.*, Interplay between copper redox and transfer and support acidity and topology in low temperature NH<sub>3</sub>-SCR, *Nat. Commun.*, 2023, **14**(1), 2633, DOI: [10.1038/s41467-023-38309-8](https://doi.org/10.1038/s41467-023-38309-8) From NLM PubMed-not-MEDLINE.
- 16 N. D. Nasello, U. Iacobone, N. Usberti, A. Gjetja, I. Nova, E. Tronconi, R. Villamaina, M. P. Ruggeri, D. Bounechada and A. P. York, Investigation of low-temperature OHC and RHC in NH<sub>3</sub>-SCR over Cu-CHA catalysts: effects of H<sub>2</sub>O and SAR, *ACS Catal.*, 2024, **14**(6), 4265–4276.
- 17 N. Ottinger, Y. Xi, C. Keturakis and Z. G. Liu, Impact of water vapor on the performance of a Cu-SSZ-13 catalyst under simulated diesel exhaust conditions, *SAE Int. J. Adv. Curr. Pract. Mobil.*, 2021, **3**(2021-01-0577), 2872–2877.
- 18 Y. Wu, Y. Ma, Y. Wang, K. G. Rappe, N. M. Washton, Y. Wang, E. D. Walter and F. Gao, Rate Controlling in Low-



- Temperature Standard NH<sub>3</sub>-SCR: Implications from Operando EPR Spectroscopy and Reaction Kinetics, *J. Am. Chem. Soc.*, 2022, **144**(22), 9734–9746, DOI: [10.1021/jacs.2c01933](https://doi.org/10.1021/jacs.2c01933) From NLM Medline.
- 19 R. Millan, P. Cnudde, V. Van Speybroeck and M. Boronat, Mobility and reactivity of Cu<sup>+</sup> species in Cu-CHA catalysts under NH<sub>3</sub>-SCR-NO<sub>x</sub> reaction conditions: insights from AIMD simulations, *JACS Au*, 2021, **1**(10), 1778–1787.
- 20 A. L. Marten and S. C. Newbold, Estimating the social cost of non-CO<sub>2</sub> GHG emissions: Methane and nitrous oxide, *Energy Policy*, 2012, **51**, 957–972.
- 21 M. P. Ruggeri, I. Nova, E. Tronconi, J. A. Pihl, T. J. Toops and W. P. Partridge, *In situ* DRIFTS measurements for the mechanistic study of NO oxidation over a commercial Cu-CHA catalyst, *Appl. Catal., B*, 2015, **166**, 181–192.
- 22 Y. Zhang, Y. Peng, J. Li, K. Groden, J.-S. McEwen, E. D. Walter, Y. Chen, Y. Wang and F. Gao, Probing Active-Site Relocation in Cu/SSZ-13 SCR Catalysts during Hydrothermal Aging by *In Situ* EPR Spectroscopy, Kinetics Studies, and DFT Calculations, *ACS Catal.*, 2020, **10**(16), 9410–9419, DOI: [10.1021/acscatal.0c01590](https://doi.org/10.1021/acscatal.0c01590).
- 23 A. Wang, Y. Chen, E. D. Walter, N. M. Washton, D. Mei, T. Varga, Y. Wang, J. Szanyi, Y. Wang and C. H. F. Peden, *et al.*, Unraveling the mysterious failure of Cu/SAPO-34 selective catalytic reduction catalysts, *Nat. Commun.*, 2019, **10**(1), 1137, DOI: [10.1038/s41467-019-09021-3](https://doi.org/10.1038/s41467-019-09021-3) From NLM PubMed-not-MEDLINE.

